JOURNAL OF SYNCHROTRON RADIATION

Volume 26 (2019)

Supporting information for article:

High pressure and temperature spinning capillary cell for *in situ* synchrotron X-ray powder diffraction

Edmundo Fraga, Armando Yáñez, Jesus D. Zea-Garcia, Angeles G. De la Torre, Ana Cuesta, Ricardo Valcárcel-Fernández, Francesc Farré-París, Marc Malfois and Miguel A. G. Aranda

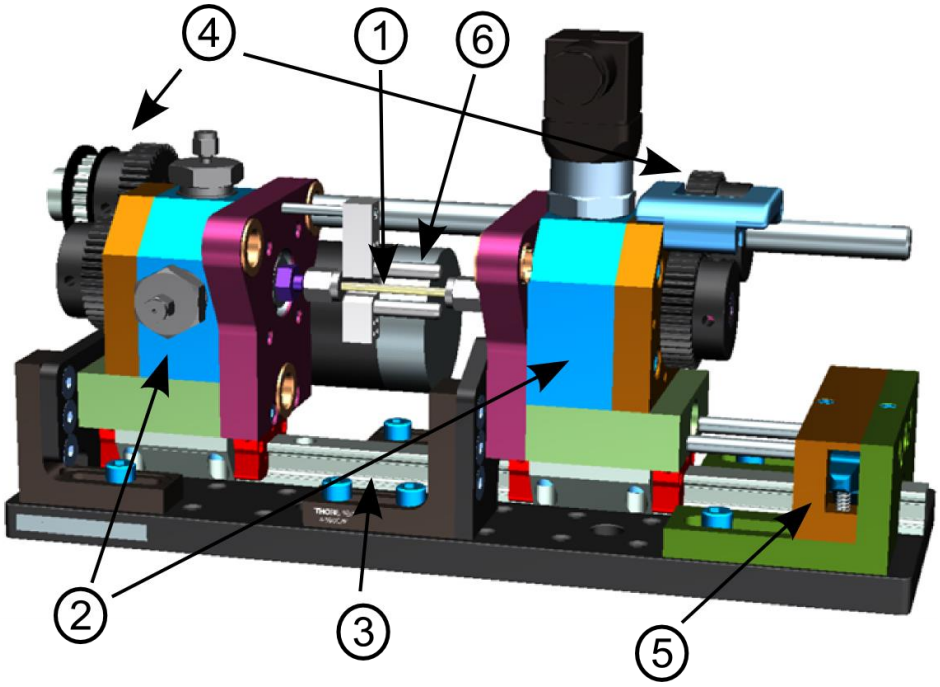

Figure S1. General description of the main components of the spinning cell over the 3D design. Main components: 1. Sample holder (removable capillary). 2. Side supports. 3. Linear displacement system. 4. Transmission system. 5. Spring lock system. 6. Heating system.

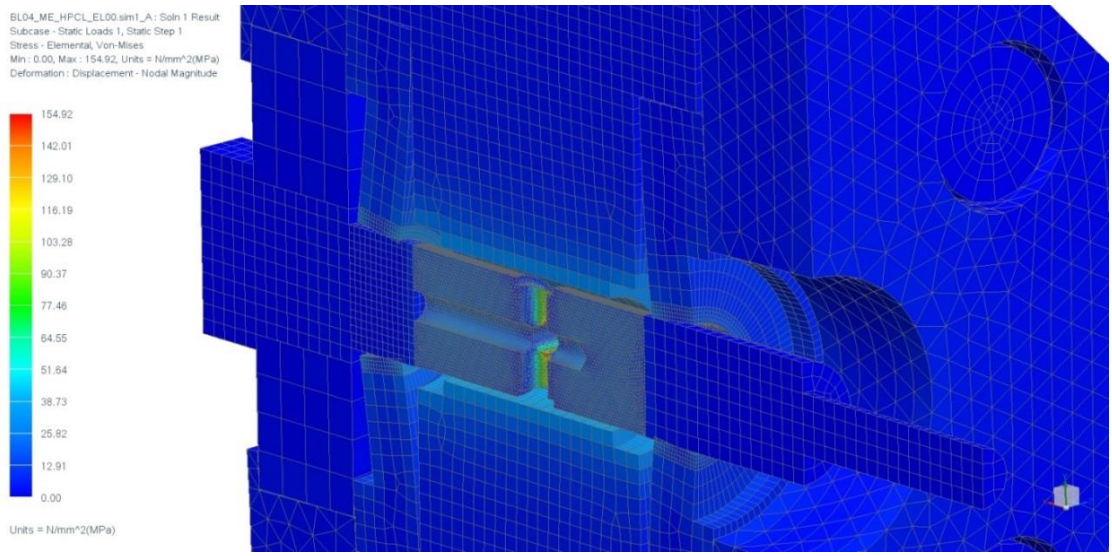

Figure S2. Equivalent tensile stress results from the Finite Element Analysis. All the stresses are below the yield strength limit. The highest stresses are very localized and coincident with the sharp edges on the entrance to the main axis, being the rest of the locations negligible when compared to the yield strength limit.

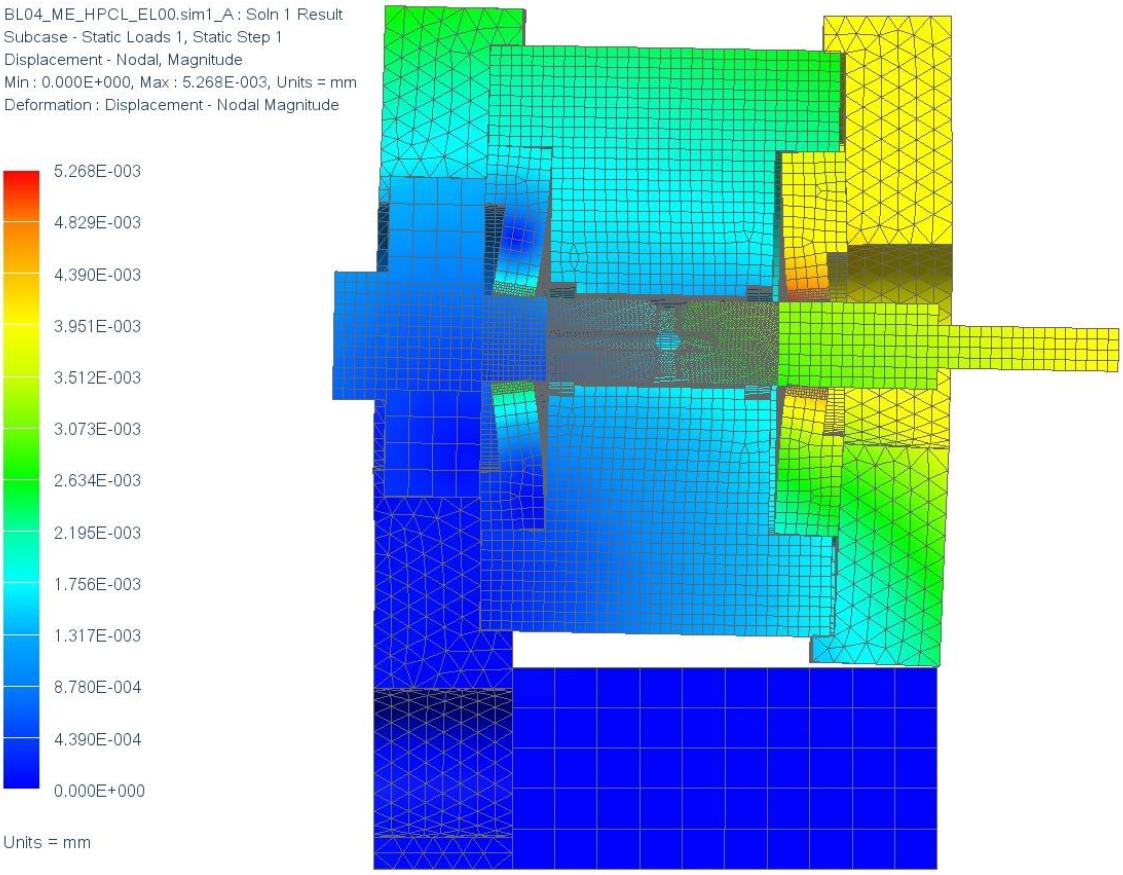

Figure S3. Nodal displacement results from the Finite Element Analysis. The pressure applied inside the exchange chamber is 20 MPa (200 bars) and the image has a deformation scale factor of 200 % of the absolute value in order to visualize the deformed mesh.

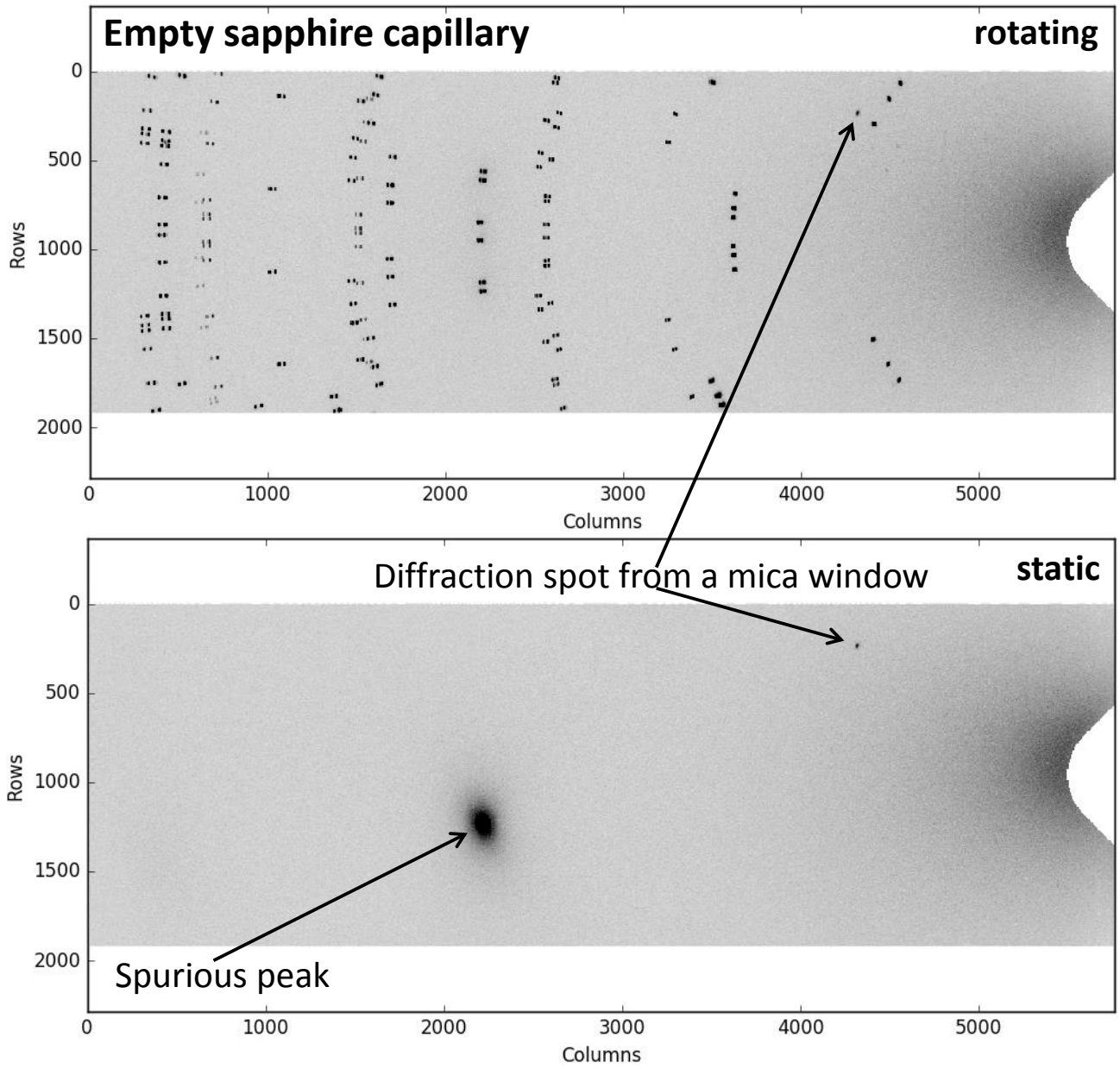

Figure S4. 2D powder diffraction patterns of the empty sapphire capillary, (top) rotating and (bottom) static. Diffraction spots from the sapphire are evident in the top pattern, at the expected position from its crystal structure. It can also be noted that sapphire diffraction peaks are split because the two walls of the capillaries are at different distances to the detector.

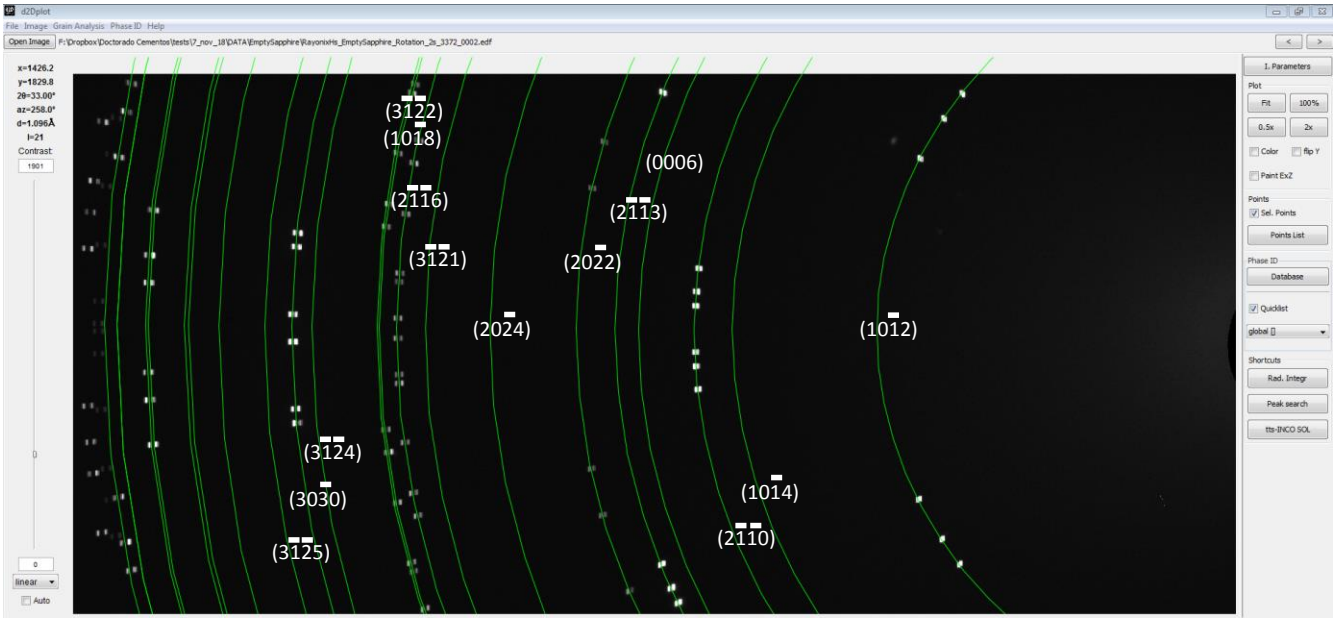

Figure S5. 2D powder diffraction patterns of the empty sapphire capillary (white spots) with the calculated corundum powder pattern (green lines) listing the Miller indexes.

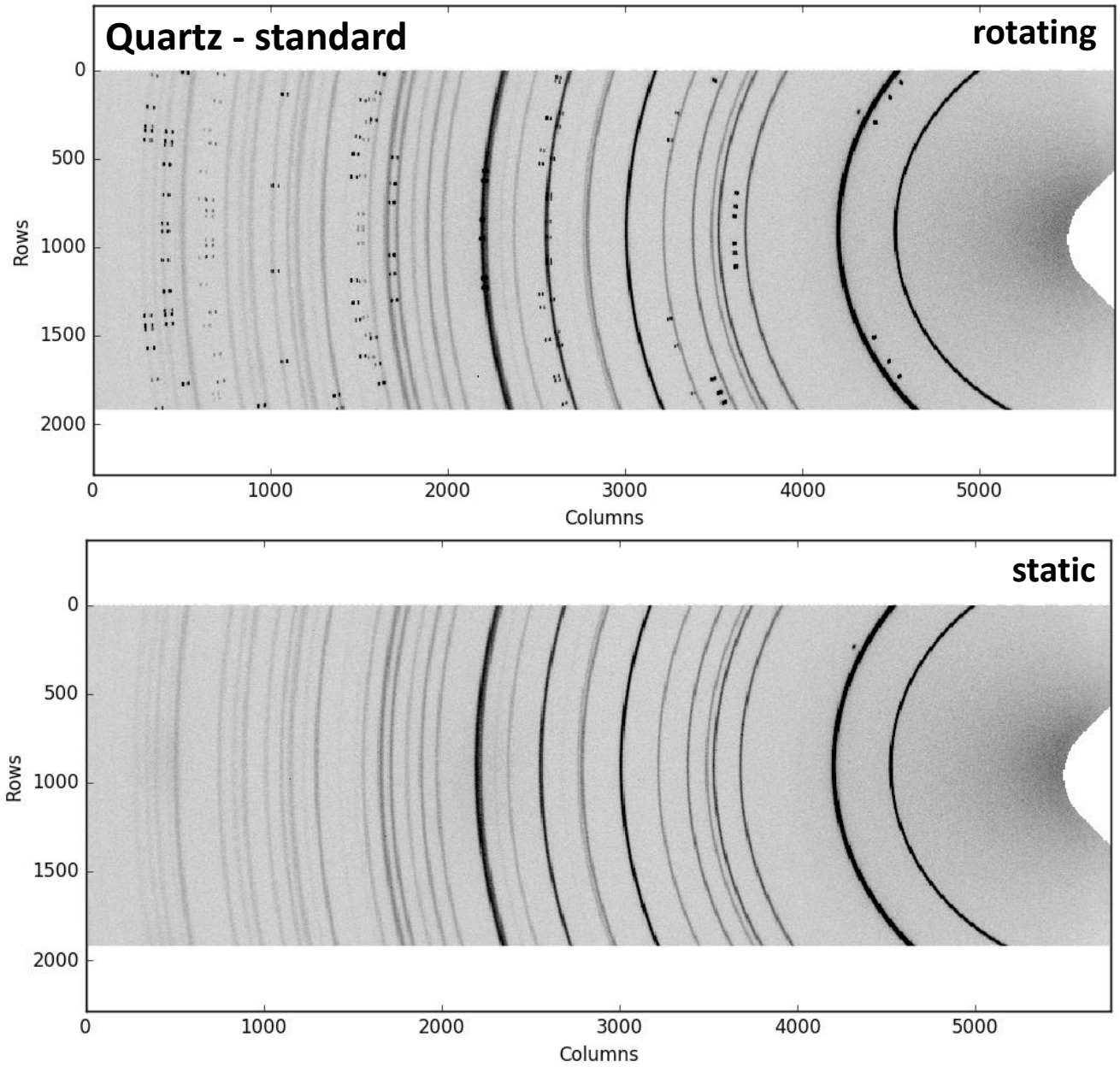

Figure S6. 2D powder diffraction patterns of the capillary filled with quartz used as standard at room temperature and pressure, (top) rotating and (bottom) static.

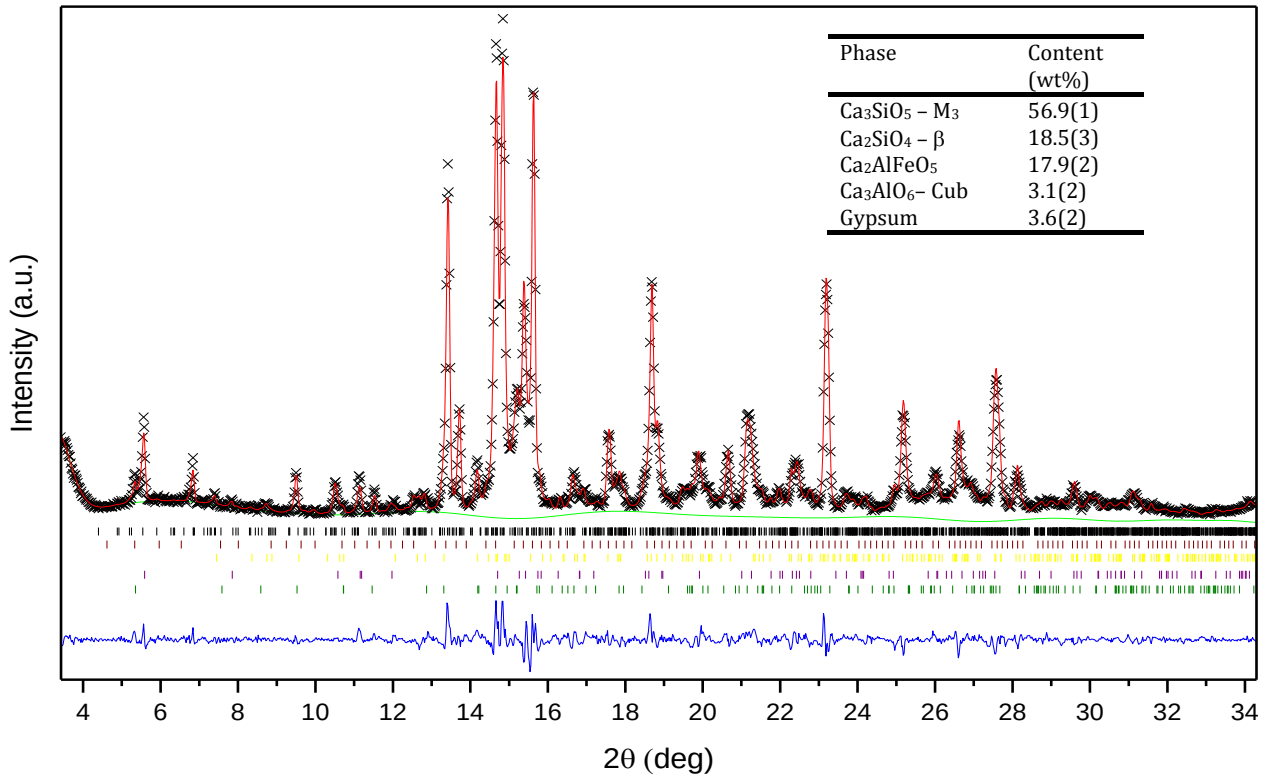

Figure S7. Rietveld plot for the laboratory X-ray powder diffraction pattern of the as-received oil well cement (Mo $K\alpha_1$ radiation). Rietveld quantitative phase analysis results are given in the inset.

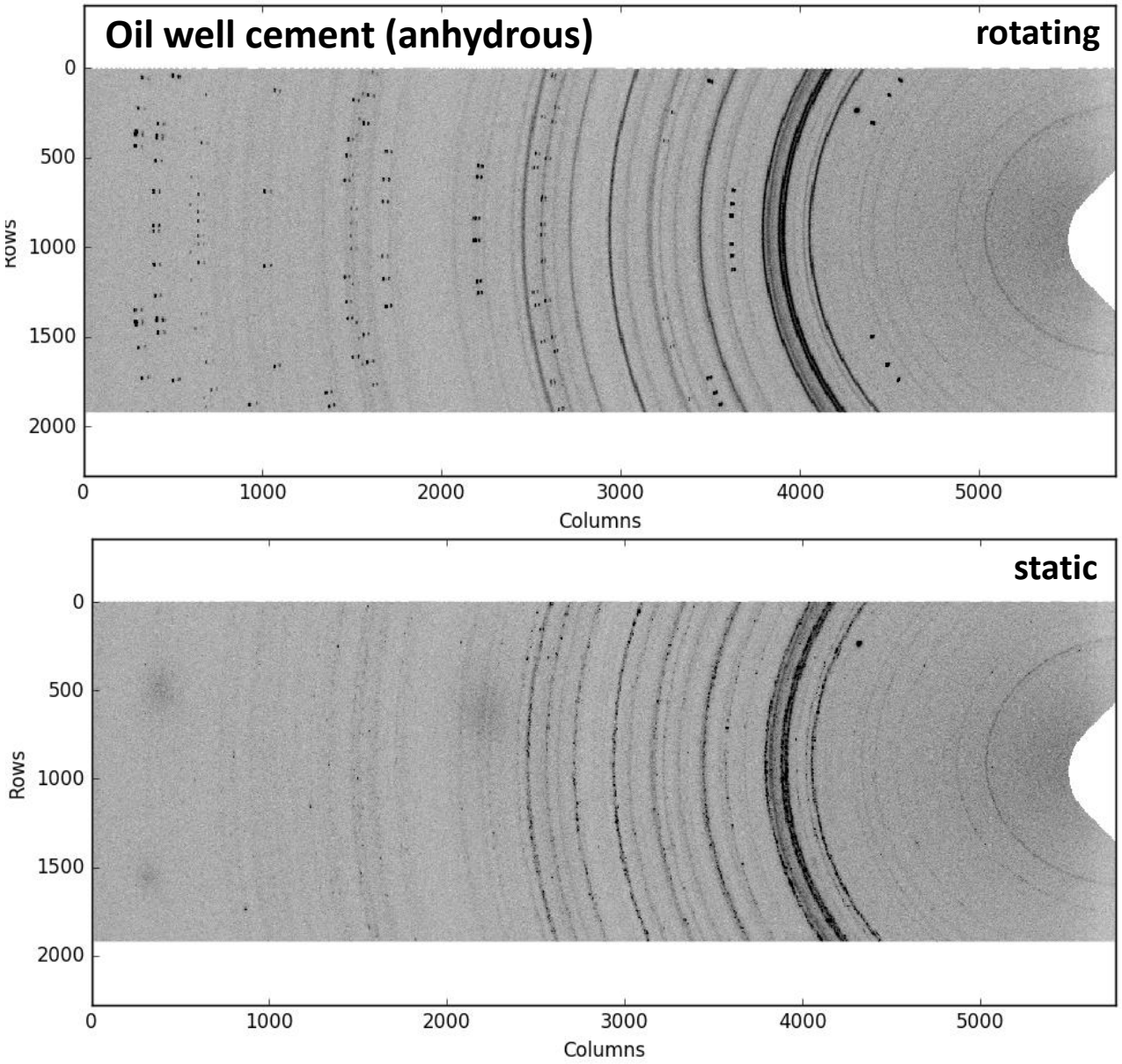

Figure S8. 2D powder diffraction patterns of the oil well cement (anhydrous) at room temperature and pressure, (top) rotating and (bottom) static.

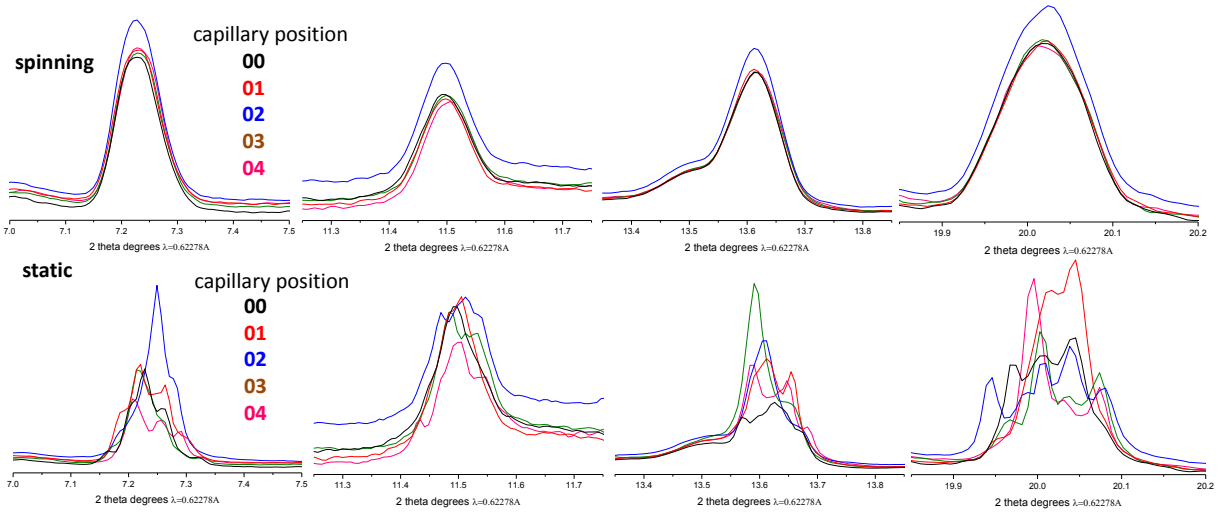

Figure S9. Comparison of the 1D synchrotron powder diffraction peaks at five capillary positions, after radial integration, for hydrating cement slurry at 14 hours, (top) rotating and (bottom) static. The evolution with 2θ is highlighted for four selected regions.